A versatile system for *in-situ* speckle and thermography-based diagnostics of artifacts

IOP Conf. Series: Materials Science and Engineering **364** (2018) 012063 doi:10.1088/1757-899X/364/1/012063

A versatile system for *in-situ* speckle and thermography-based diagnostics of artifacts

L Perlini[1], D Ambrosini[2,3] and C Daffara[1,3]

[1] University of Verona, Dept of Computer Science, Strada Le Grazie 15, Verona (VR), Italy
[2] University of L'Aquila, DIIIE, Piazzale Pontieri 1, Monteluco di Roio (AQ), Italy
[3] CNR - Institute of Applied Science & Intelligent Systems, via Campi Flegrei 34, Pozzuoli (NA), Italy

E-mail: luca.perlini@univr.it

Abstract. Holographic nondestructive techniques already showed their effectiveness in detecting structural defects on or beneath the surface of historical artifacts, not emerging from conventional visual inspections. Unfortunately, such tools are difficult to be operated out of the stability conditions guaranteed by an optics laboratory. The peculiar features of many works of art, however, make often impracticable their transport to dedicated facilities. In this work, a compact, stable, portable holographic system was designed and implemented: the resulting apparatus allows *in-situ* acquisitions, even in non-laboratory conditions, and provides rapid and clearly interpretable diagnostic information by the completely non-invasive procedure of speckle pattern photography (SPP). Complementary data are furnished by an integrated infrared thermography system. A map of the artifact surface can be obtained, representing the distribution of defects and their extension. The technique will hopefully help or replace conventional methods, more invasive or less systematic (visual inspections, surface tapping), still largely used for the same purposes.

1. Introduction

Historical artifacts undergo, with time, structural alterations induced by aging and by the interaction with the environment [1, 2]. Daily and seasonal variations of temperature and humidity expose every artwork to cyclic stresses which, associated to the progressive weakening of the constitutive materials, can lead to irreversible damage on or beneath the surface of the specimen.

Artistic supports presenting highly layered structures, such as paintings or *frescoes*, are especially susceptible to the onset of detachments, voids, microcracks and delaminations, in consequence of the decay process. A detailed evaluation of aging-induced defects and a monitoring of their evolution are required to guide the restorers' work and to prevent major damages, especially in the presence of possible drastic triggering events, like earthquakes.

Beside conventional investigation techniques (visual inspections, surface percussion, etc.), still largely used to this aim, a number of systematic, reliable and non invasive tools are provided by optical techniques [3, 4].

Surface holography, and in particular speckle-based methods, already showed their effectiveness in detecting sub-superficial defects – thus invisible to the naked eye – on different types of supports [2, 5]. In addition to the advantageous whole-field, high resolution and non-contact characteristics,

such techniques include algorithms for the digital analysis of images [6] providing a clearly interpretable description of the state of conservation of the artwork in rapid times.

The greatest obstacle left to the systematic application of such techniques is represented by their high sensitivity to external disturbances, like vibrations. The optimal conditions of mechanical stability are hardly reached and maintained, except that in laboratory situations [2]. Since, however, the nature of many artifacts makes inadvisable or impossible their transport to dedicated facilities, the research in this field is now addressed to the problem of allowing *in-situ* acquisitions.

Speckle digital methods, like electronic speckle interferometry (ESPI) [6, 7] and speckle photography (SPP) [7, 8], are able to meet this need.

In this article, a particularly simple, compact, easy-to-transport and accessible speckle-based setup was implemented, characterized and optimized for the research of sub-superficial detachments on paintings and *frescoes*.

Considering the complex structure of works of art, a number of studies [9–12] suggested the integration of non-invasive, complementary and independent tools, in order to reach complete diagnostic information. The proposed setup was thus integrated with a compact infrared thermography system, acquiring data from the sample at the same time as the speckle system.

2. Basic Principles

A detached region beneath the surface of a painting does not emerge from a simple visual inspection, but can reveal its presence when the artwork is thermally stressed. In correspondence of the detachment, the lack of adhesion reduces the heat dispersion rate and slows down the return to equilibrium conditions. This translates into two observable surface effects: an anomalously high temperature in that location; and an irregular deformation field, both in intensity and in time persistence.

2.1. Speckle Methods

Speckle effect arises when a coherent radiation field hits a rough diffusing surface [8, 13]. Many secondary spherical wavelets are back-scattered, and the optical interference between different contributions creates a granular pattern on the surface. The geometry of the speckles strongly depends on the imaging system used for the observation [7, 8].

A relation holds between such pattern – which can be described in statistical terms [13] – and the micro-morphology of the surface. In particular, every deformation of the latter results in a modification of the corresponding speckle pattern. Such correspondence is maintained down to displacements in the order of multiples of the radiation wavelength, namely to the micrometer scale. Moreover, a "locality" principle is satisfied [14]: a local deformation of the surface causes a local deformation of the speckle pattern in that precise location.

Such properties constitute the basis of speckle metrology, which investigates shape and deformations of a surface by acquiring and comparing speckle patterns in sequence. Two are the principal approaches, both based on digital acquisition and analysis procedures [6].

Speckle interferometry (ESPI) involves a two-beam configuration analogue to the traditional holographic interferometry, and found advantageous application in the conservation field [15–20]. However, it requires some stability conditions and the presence of an optics-skilled specialist to be operated [21].

The information about some particular components of the surface displacement field is accessible even in the absence of the reference beam [8]. In this case, the speckle pattern generated by the object beam alone, which is called a specklegram, is acquired. Comparative correlation analyses of successive specklegrams from the same surface, before and after an external *stimulus*, allow to measure the involved deformation field. Such one-beam option, called Speckle Pattern

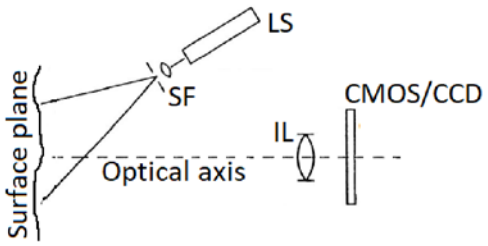

Figure 1: Schematic SPP setup. LS: laser source; SF: spatial filter; IL: imaging lens.

Photography (SPP), is especially sensitive to in-plane displacement components and local tilting [8], within the range $10^1 \div 10^3$ µm.

Despite these limits, the final setup, the acquisition procedure and the stability requirements turn out to be very simplified, if compared to ESPI, making conceivable a compact dedicated apparatus, suitable for *in-situ* campaigns and operable by non-scientists too. A scheme of a typical SPP setup is reported in Figure 1.

Laser speckle is not limited to reflected light geometry: the same effect arises when coherent light is transmitted through a diffuser medium, such as a ground glass [13]. In the image of such medium, projected on the inspected surface, strong fluctuations in intensity are observed, caused by the superposition of secondary wavelets generated and dephased inside the diffuser.

2.2. Infrared Thermography

A radiometric system measures the energy of the electromagnetic radiation emitted by a surface and correlates it to its temperature, following the relationship between the two quantities provided by Plank's blackbody theory. In the case of objects around the room temperature – the ones which conservation deals with – the theory provides the emission peak to fall in the far-infrared (FIR) interval ($7 \div 14$ µm).

The employment of such technique as a diagnostic tool is made possible by the fact that the actual thermometric response of a real object, like an artifact, is influenced by a number of properties: spectral (emissivity, absorption, reflection), thermal (conductivity, diffusivity, specific heat) and general physical conditions, including but not limiting to porosity, water content and surface treatment. Ultimately, the presence of a structural defect alters locally one or more of such properties, and hence the emission regime. It is thus possible to detect and map the thermal variations of a work of art and correlate them to the material conditions, to its microstructure and to the morphology of its surface [1].

In the so-called *active* approach [22], an external source, generally in the form of a pulsed heat *stimulus*, is used to create thermal contrast. Again, a detached region is associated to a lower heat transfer rate and a higher temperature with respect to the surrounding regions, and it is revealed as a thermal discontinuity on the artifact surface.

Among the advantages offered by IRT, non-contact and full-field features must be mentioned, together with rapid acquisition times and clearly interpretable results [22]. On the other hand, the difficulty to obtain a uniform thermal solicitations of wide areas and the uncertainty about the emissivity and reflectance of composite materials are the most critical points to deal with.

3. Experimental Setup

The proposed setup is schematically reported in Figure 2. Its design favors compactness and modularity, and allows fine components adjustments without affecting the alignment of non-involved parts. In the present study, the system was optimized for speckle photography measurements (in one-beam geometry) together with thermography.

Speckles produced in transmission configuration are largely exploited in the present work, since they lead to some practical advantages: the speckle field is projected onto a very wide area (in

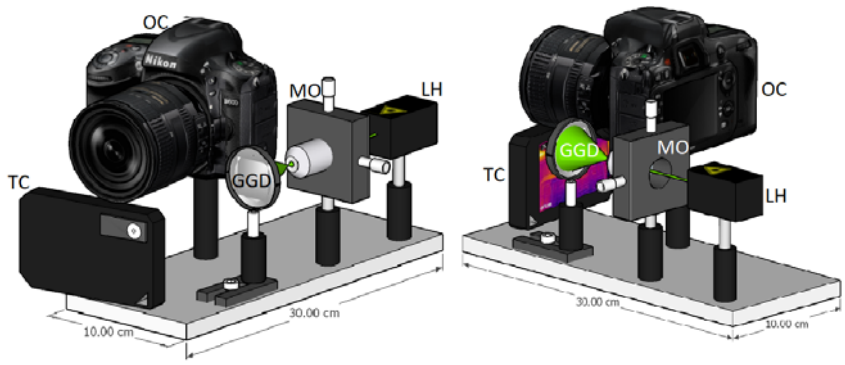

Figure 2: 3D model of the proposed apparatus. LH: laser head; MO: microscope objective; GGD: ground glass diffuser; OC: optical camera; TC: thermal camera. Approximate total weight: 3 kg. The supporting optical breadboard can be mounted on a stiff photographic tripod.

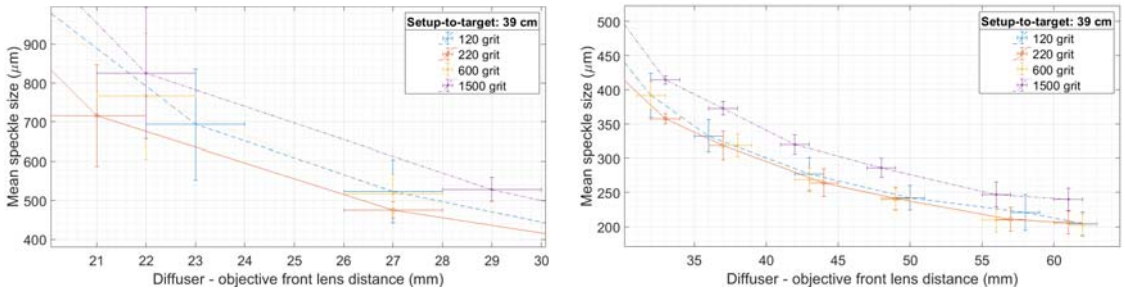

(a) (b)

Figure 3: Mean speckle dimension as a function of the diffuser grain and of its distance from the front element of the microscope objective. The calibration curve also depends on the distance between the sample and the diffuser: in this case, such parameter is 39 cm.

the order of 1 m^2) in a uniform way and it is barely subject to distortions or aberrations induced by the beam-expander. Moreover, the mean speckle size is generally increased, decreasing the sensitiveness to displacement but relaxing the resolution requirements for the acquisition phase.

The coherent light source is provided by a DPSS laser with output wavelength of 532 nm and maximum power of 125 mW. The chosen operative power depends on the background illumination conditions and on the nature of the sample: a number of tests suggested powers in the range $60 \div 90$ mW.

Sensitiveness to displacements is reached even if the laser beam impinging on the surface is divergent [8]. Therefore, an Olympus Plan-N 10x/0.25 microscope objective is used as a beam expander: this solution guarantees very high enlargement and allows to illuminate a wide area.

A ground glass diffuser is placed after the objective to operate in transmission geometry. The distance between these two components determines the speckle dimension (and thus, for the greatest part, the minimum spatial resolution): in order to have such dependence under control, the mean speckle size was measured for varying diffuser grain level and distances from the objective front lens. As observable from the graphs in Figure 3, both factors concur to the final speckle size, which is included, for this particular setup, in the range $150 \div 700$ µm.

The three components addressed to surface illumination are fixed on a 10×30 cm optical breadboard, together with a CMOS camera (Nikon D810, $7360 \times 4912 \times 14$ bits) mounting a 50 mm imaging lens with aperture in the range from f/9 to f/11. A green band-pass filter on the front part of the lens limits the background light collected on the sensor. The camera, used to

acquire the specklegrams of the surface before and after the thermal stress, is remotely controlled by computer – as well as the laser source – in order to avoid direct interventions of the operator during the acquisition.

A bolometer-based thermal camera (FLIR C2) is mounted on the breadboard, just in front of the optical camera (see Figure 2). This model of infrared camera is characterized by a very compact design, which makes it suitable to be integrated in the system without affecting its overall geometry. The device provides access to the raw radiometric data, allowing the correct estimation of temperature also in the complex situation of surfaces with heterogeneous emissivity or in presence of reflections. Moreover, it can be operated in streaming mode with a computer via USB connection.

The whole setup is protected from mechanical disturbances and vibrations by a set of sorbothane feet.

The resulting system can be laid on a scaffolding plane; alternatively it can be mounted on a stiff photographic tripod, at variable distance from the inspected surface. After some tests, the optimal distance for acquisitions of projected speckles was estimated about 40 cm, corresponding to a 20 cm diameter ROI.

The thermal *stimulus* is provided by a 750 W infrared tungsten lamp pointed toward the front surface of the artifact (the inspected one) from a distance of 40 cm. The collected data are referred to long-pulsed solicitations of variable duration, between 5 and 30 s.

4. Digital image processing

The local surface displacement is deduced from that of the two speckle patterns, acquired before and after the external solicitation. The comparison between them is performed by computer algorithms, usually based on cross-correlation calculations. Basic assumption of the diagnostic process is that defective subregions are identified by local irregularities in the direction or in the intensity of the average displacement field. In particular, since a SPP setup is especially sensitive to in-plane deformations, such regions correspond to places in which the initial speckle pattern undergoes an anomalously high translation, when compared to the surrounding. Within this region, the correlation between the two specklegrams drops.

Our analysis relies on the adaptation of two Matlab scripts, based on quite different approaches. In both cases, the raw speckle images are pre-processed for contrast enhancement, exposure fluctuations and vibrations compensation and for cutting any residual contribution from background radiation. Since we operate in green laser light illumination, the red and blue channels of every image are put to zero.

The Speckle Correlation (SC) method consists in the evaluation of a local parameter, estimating the correlation of the speckle patterns after the modification of a surface element: it was applied, in the past, during similar studies on different artistic supports (wooden paintings, mosaics and *frescoes*). Calling, respectively, $u_{\mathrm{ref}}(x,y)$ and $I_{\mathrm{ref}}(x,y)$ the field amplitude and intensity relative to the surface in its initial state, and $u_{\mathrm{mod}}(x,y)$ and $I_{\mathrm{mod}}(x,y)$ the same quantities after the solicitation, a local correlation coefficient is defined as [13, 23]

$$\rho(x,y) = \frac{|\,\langle u_{\mathrm{mod}}(x,y) u^{*}_{\mathrm{ref}}(x,y)\rangle\,|^2}{\langle I_{\mathrm{mod}}(x,y)\rangle\,\langle I_{\mathrm{ref}}(x,y)\rangle} \tag{1}$$

Under some statistical assumptions about the signal and about the linear response of the camera, it was demonstrated [13] that $\rho(x,y)$ can be obtained from the spatial average of the squared arithmetic difference of the two specklegrams, according to [23]

$$\rho(x,y) = 1 - \frac{\langle [I_{\mathrm{ref}}(x,y) - I_{\mathrm{mod}}(x,y)]^2\rangle}{\langle I^2(x,y)\rangle} \tag{2}$$

where the angle brackets denote a spatial local average, executed over an area containing many speckles. Eq. (2) ensures that subtracting the displaced specklegram from the reference one, squaring the result, averaging over many speckles and dividing by a normalization factor, the complement-to-one of the correlation parameter is obtained. Thus, in the resulting image, bright areas represent regions of higher decorrelation, associated to strong in-plane displacement fields, and thus to the presence of detached layers or other types of defect. Practically, local averaging is effected by a discrete convolution between the gray-scale image and a matrix of ones, dimensioned such to contain a statistically significant number of speckles.

A quantitative geometrical reconstruction of displacement can instead be reached by adapting Particle Image Velocimetry (PIV) tools [9]. One example is provided by MatPIV, developed in the Matlab environment [24]. It receives as input the two specklegrams, which are divided into sub-images of dimensions set by the user. Every sub-region from the undisplaced image is associated to the corresponding one from the displaced image through a cross-correlation calculation, and an average in-plane displacement vector is constructed in each window. The FFT algorithm is exploited in the calculation to speed up the running time, which remains in the order of some minutes even for inexpensive computers. A detailed description of the software functioning is provided in its documentation (see [24]). In our case, cross-correlation is calculated with one iteration through the images and a 50% overlap of the interrogation windows.

5. Results and Discussion

In order to evaluate the effectiveness of the proposed setup in detecting hidden detachments, a plausible diagnostic procedure was carried out on a specimen with known structure. A sample model of 60×40 cm was realized, reproducing the layered structure typical of Renaissance paintings. The choice of materials and fabrication methods was guided by *Il libro dell'arte* by Cennino Cennini, one of the main treatises about the sixteenth-century paintings techniques. At various levels of the pictorial support – based on linen stripes fixed on a poplar table by a series of successive hands of Bologna chalk and rabbit-skin glue mixture – a number of plastic leafs were inserted, in order to impede adhesion between adjacent layers and simulating the effect of aging-induced detachments. Insertions differed from each other in dimension, position and depth.

The intensity of the external thermal *stimulus* was also varied. The long-pulse duration of the IR source was progressively increased from 5, to 15, to 30 s: the superficial temperature of the sample was measured by the thermal camera in real-time. As recommended for these type of solicitation on very fragile artifacts [3, 16], the temperature gradient did not exceed values of $4 \div 5\,^{\circ}$C. The post-*stimulus* specklegrams were acquired both at the top of the heating and during the cooling phase, respectively after 5 and 65 s from the lamp switching-off.

Some results are shown in Figure 4. When comparing the reference specklegram with the one acquired during the cooling phase (65 s after the lamp switching-off), the SC-based software gives an account of a bright area – and thus very decorrelated – correspondent in position and dimension to the defective one (Figure 4c). Other partially decorrelated regions are detected, not associated with the presence of underlying plastic sheets: it is possible for such "false positives" to arise as a consequence of a non-uniform external solicitation or of an unexpectedly unstable part of the sample. No comparable effectiveness seems to be obtained when acquiring the displaced specklegram at the top of the heating phase, as shown in Figure 4b, in which no contrast enhancement could be performed.

Figures 4d and 4e show the results of the MatPIV-based analysis. The script was adapted to visualize only the local displacement outliers, i.e. the subregions in which the deformation underwent abrupt direction or intensity changes with respect to the surrounding and to the average of the ROI. The same area as before is recognized as defective, presenting a very high concentration of anomalous displacement vectors. In general, a wide irregular field is reconstructed all over the bottom part of the investigated area: the most likely explanation is analogue to that

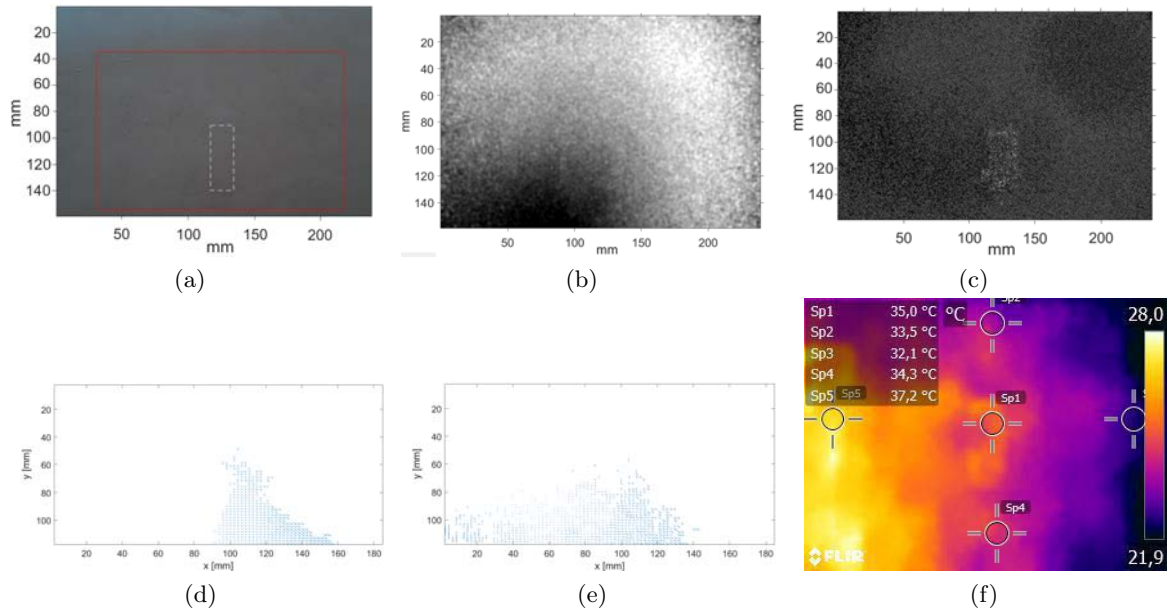

(a) (b) (c)

(d) (e) (f)

Figure 4: (a): Investigated ROI. The dashed rectangle locates the detachment, the solid red one indicates the region analyzed by MatPIV. Laser output power: 60 mW; exposure time: 1/5 s; aperture: f/11.0; surface temperatures (pre-*stimulus*, 5 s post-*stimulus*, 65 s post-*stimulus*): $T_0 = 23.5 \pm 0.5\,^{\circ}\mathrm{C}$, $T_1 = 26.7 \pm 0.5\,^{\circ}\mathrm{C}$, $T_2 = 25.5 \pm 0.5\,^{\circ}\mathrm{C}$. (b)-(e): SC and MatPIV speckle displacement data relative to a thermal *stimulus* of 5 s duration. Displaced specklegram acquisition: (b),(d): 5 s and (c),(e): 65 s after the lamp switching-off. (f): Thermographic data relative to a 30 s-lasting *stimulus*.

provided for the SC analysis.

Two indications can be extracted from the data. First, that the presence of a defect is most likely to emerge when a "response time" is waited after the end of the *stimulus*, before acquiring the displaced specklegram. This fact, already established by similar studies [3], is explained by recalling that, during the redistribution of thermal energy from the surface to the bulk, detached areas undergo anomalous heat accumulations, and thus deformations more persistent in time. Maximum contrast is then generated, during the cooling phase, with the regular regions, which instead return faster to the equilibrium situation. Second, that a more intense *stimulus* is not necessarily associated to higher defects detectability; a fact that is useful to further reduce the potential invasiveness.

Thermographic data from the same ROI are presented in Figure 4f. The detachment emerges, as expected, as a region with higher temperature than the surrounding.

6. Conclusions

In this work a speckle imaging setup for the diagnostics and evaluation of historical paintings was proposed, characterized by portability, modularity and suitability for *in-situ* measurement campaigns. The adopted hardware and software solutions provided a tool sensitive to the presence of hidden sub-superficial detachments, but at the same time barely influenced by the main noise sources (vibrations and fluctuations in background radiation).

Placing side by side a speckle and a compact thermographic system optimized the measurement procedure: in fact, by exploiting an external thermal stress it was possible, during a unique cycle, to obtain complementary and independent diagnostic data from the two techniques, as well as to monitor in real time the surface temperature.

Preliminary tests proved the system to be characterized, making use of some medical terminology, by good diagnostic sensibility when applied to the research of detachments on painting-like supports. Specificity can instead be improved, for example by ensuring a very uniform thermal solicitation all over the inspected surface. A full understatement of the potentialities of the system and a characterization of the optimal measure protocol will however require other data, for example from the application to artistic supports other that paintings.

References

[1] Moropoulou A, Labropoulos K C, Delegou E T, Karoglou M and Bakolas A 2013 *Construction and Building Materials* **48** 1222–1239
[2] Ambrosini D and Paoletti D 2004 *Studies in Conservation* **49, sup. 1** 38–48
[3] Fotakis C, Anglos D, Zafiropulos V, Georgiou S and Tornari V 2006 *Lasers in the preservation of cultural heritage: principles and applications* (CRC Press)
[4] Zhu Y K, Tian G Y, Lu R S and Zhang H 2011 *Sensors* **11** 7773–7798
[5] Hinsch K D 2007 *Oscillation, Waves and Interaction* 259
[6] Rastogi P K 2000 *Digital Speckle Pattern Interferometry and Related Techniques, by PK Rastogi (Editor), pp. 384. ISBN 0-471-49052-0. Wiley-VCH, December 2000.* 384
[7] Cloud G 1998 *Optical methods of engineering analysis* (Cambridge University Press)
[8] Jones R and Wykes C 1983 *Holographic and Speckle Interferometry* second edition ed (Cambridge University Press)
[9] Ambrosini D, Paoletti D and Galli G 2008 *Lasers in the Conservation of Artworks, Proceedings of the International Conference LACONA* vol 7 pp 399–405
[10] Hinsch K D, Gülker G and Helmers H 2007 *Optics and Lasers in Engineering* **45** 578–588
[11] Ambrosini D, Daffara C, Di Biase R, Paoletti D, Pezzati L, Bellucci R and Bettini F 2010 *Journal of Cultural Heritage* **11** 196–204
[12] Daffara C, Parisotto S and Ambrosini D 2017 *Optics and Lasers in Engineering* (In Press, Corrected Proof)
[13] Goodman J W 2007 *Speckle phenomena in optics: theory and applications* (Roberts and Company Publishers)
[14] Shih Y C, Davis A, Hasinoff S W, Durand F and Freeman W T 2012 *Computer Vision and Pattern Recognition (CVPR), 2012 IEEE Conference on* (IEEE) pp 33–40
[15] Albrecht D, Franchi M, Lucia A C, Zanettaa P M, Aldrovandi A, Cianfanelli T, Riitano P, Sartiani O and Emmony D C 2000 *Journal of Cultural Heritage* **1** S331–S335
[16] Tornari V 2007 *Analytical and bioanalytical chemistry* **387** 761–780
[17] Hinsch K D, Zehnder K, Joost H and Gülker G 2009 *Journal of Cultural Heritage* **10** 94–105
[18] Lucia A C, Zanetta P M and Facchini M 1997 *Optics and lasers in Engineering* **26** 221–233
[19] Paoletti D and Spagnolo G S 1996 *Progress in Optics* **35** 197–255
[20] Krzemień L, Lukomski M, Kijowska A and Mierzejewska B 2015 *Journal of Cultural Heritage* **16** 544–550
[21] Memmolo P, Arena G, Fatigati G, Grilli M, Paturzo M, Pezzati L and Ferraro P 2015 *Journal of Display Technology* **11** 417–422
[22] Maldague X 2001 *Theory and practice of infrared technology for nondestructive testing* (Wiley)
[23] Spagnolo G S, Paoletti D, Ambrosini D and Guattari G 1997 *Pure and Applied Optics: Journal of the European Optical Society Part A* **6** 557
[24] Sveen J K 2004 *Preprint series. Mechanics and Applied Mathematics http://urn. nb. no/URN: NBN: no-23418*